Observation and modeling of solar coronal loops

Cecilia Mac Cormack

Marcelo López Fuentes, Cristina Mandrini

Instituto de Astronomía y Física del Espacio, Buenos Aires, Argentina.

February 22, 2023

Introduction

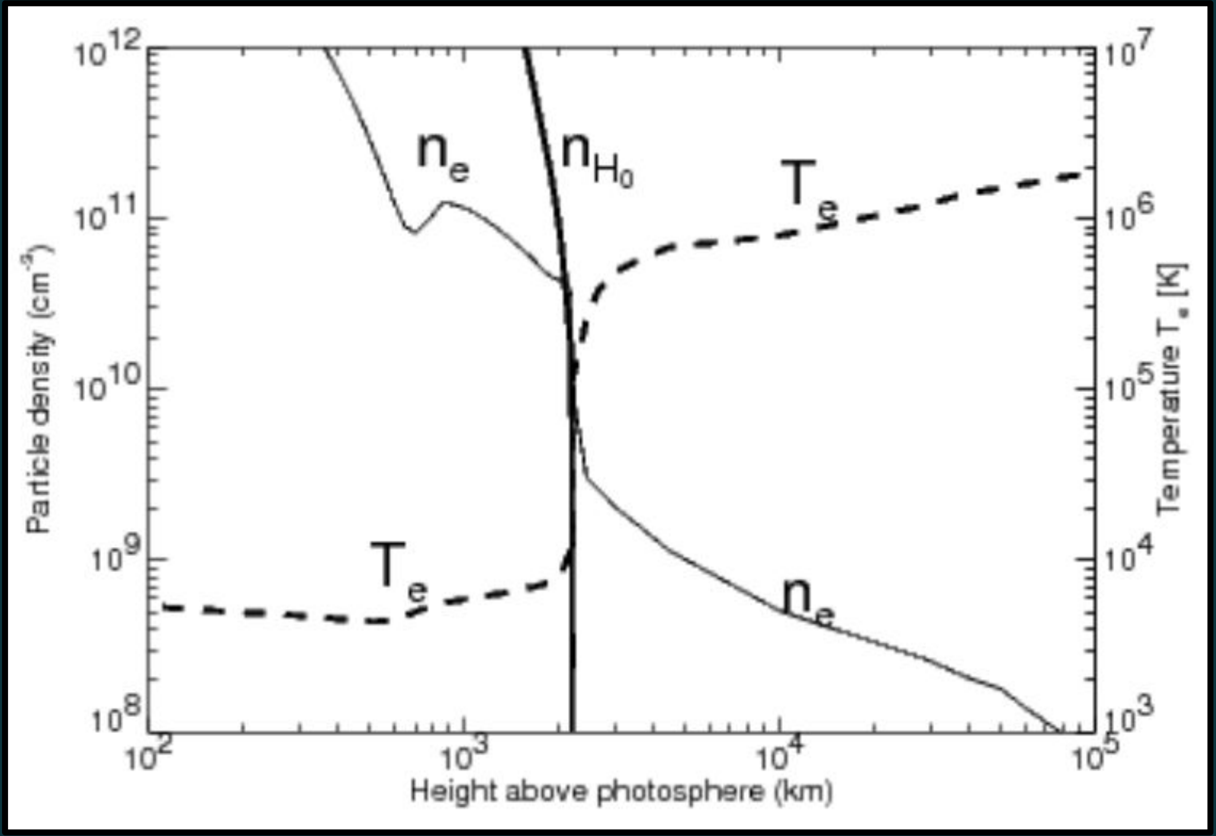

Gabriel, 1976, RSPTA, 281, p. 339.

Introduction: Solar Cycle

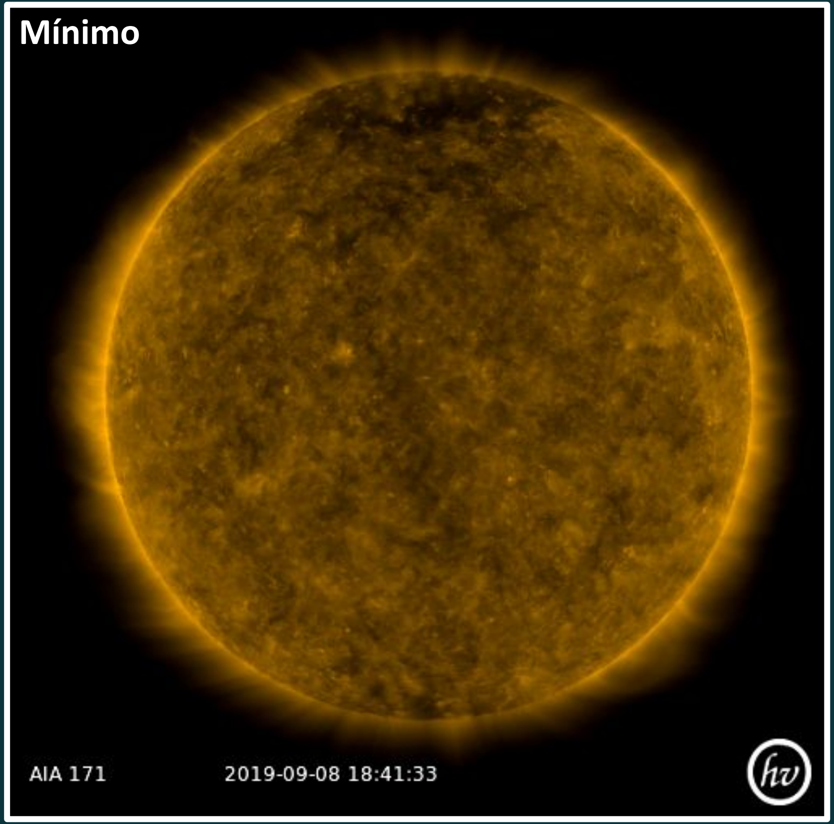

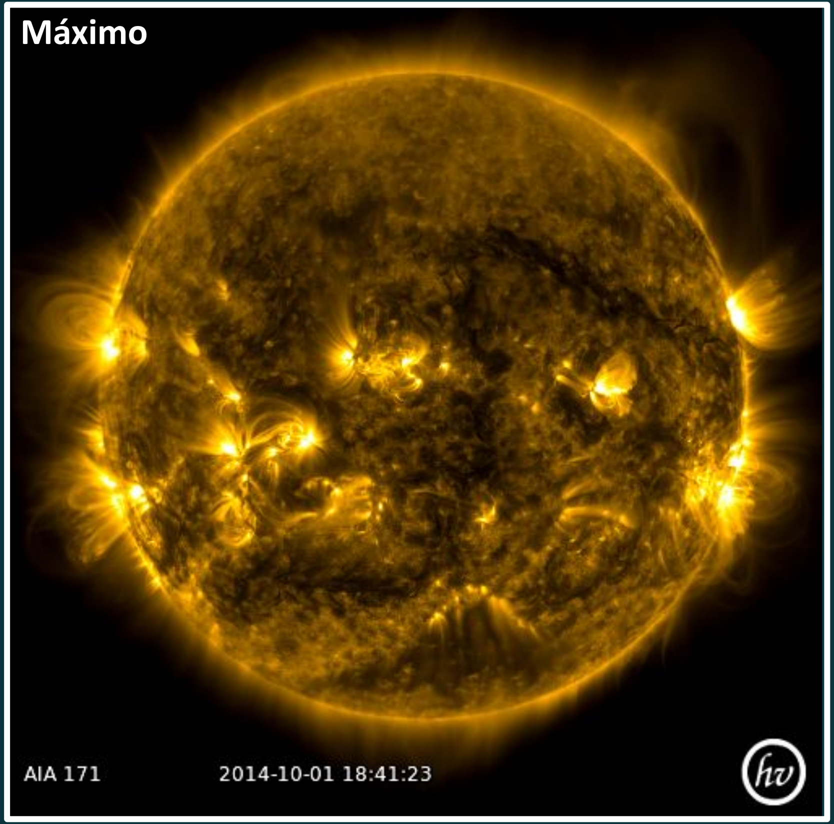

Differential emission measure tomography

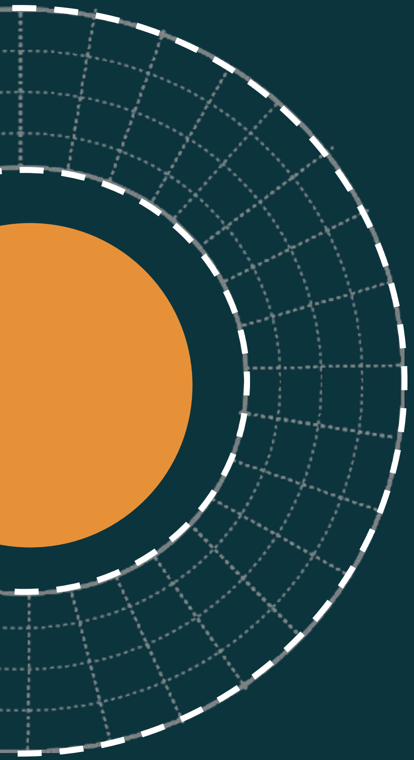

r ~ [17,157] Mm

Voxel: 2° x 2° x 14 Mm

Frazin, Vásquez & Kamalabadi, 2009, ApJ, 701, p. 547.

Differential emission measure tomography

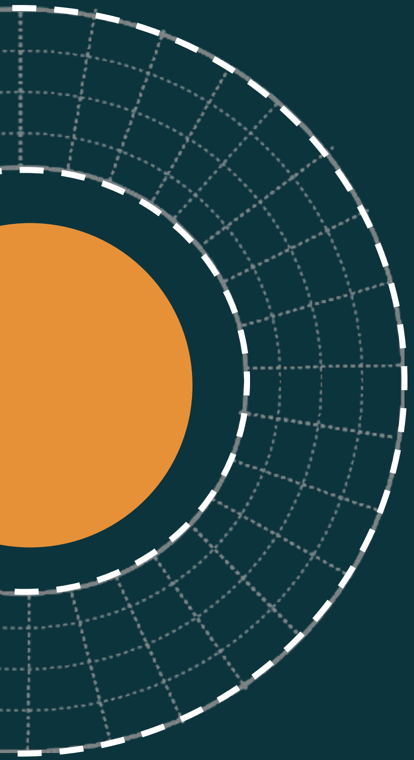

r ~ [17,157] Mm

Voxel: 2° x 2° x 14 Mm

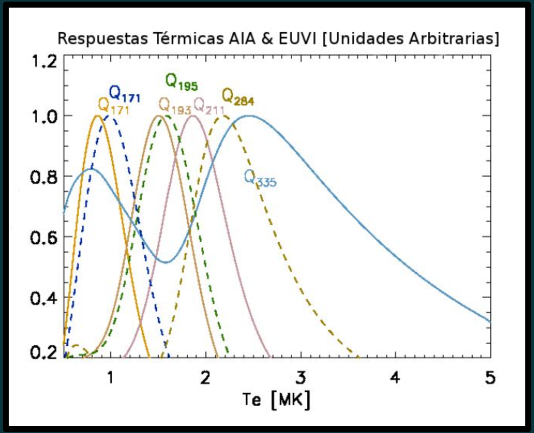

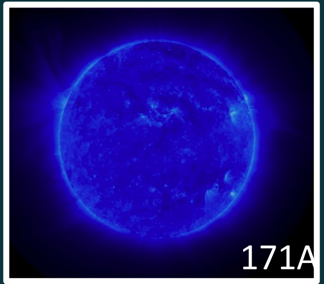

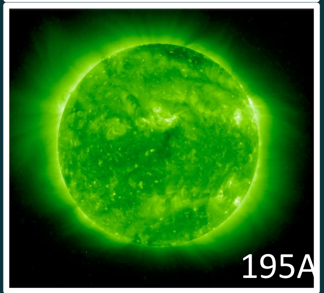

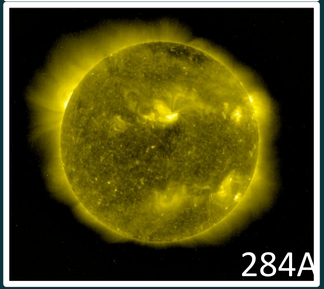

Frazin, Vásquez & Kamalabadi, 2009, ApJ, 701, p. 547.

Differential emission measure tomography technique

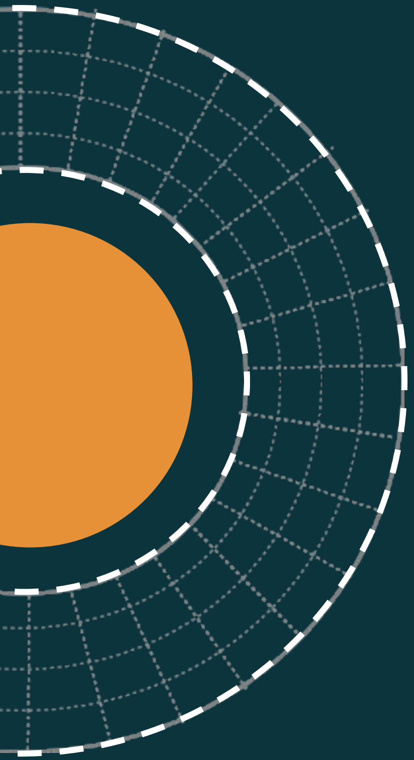

r ~ [17,157] Mm

Voxel: 2° x 2° x 14 Mm

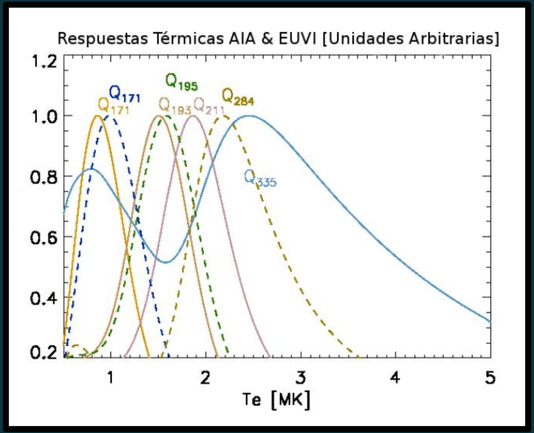

$$I_{k,j} \approx \int_{LDV} \mathrm{d}z \; \mathrm{FBE}_k(\mathbf{r}_j(z))$$

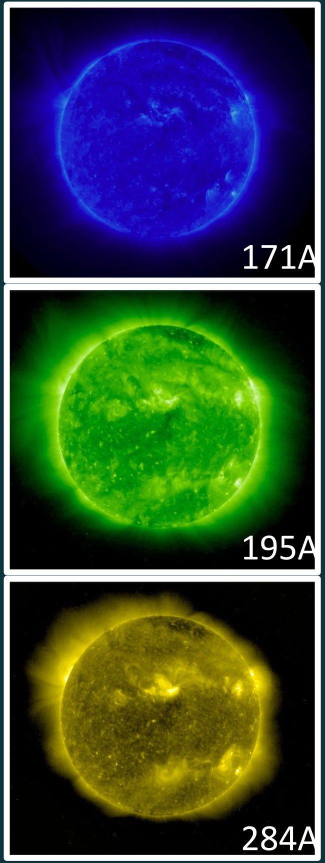

Frazin, Vásquez & Kamalabadi, 2009, ApJ, 701, p. 547.

Differential emission measure tomography technique

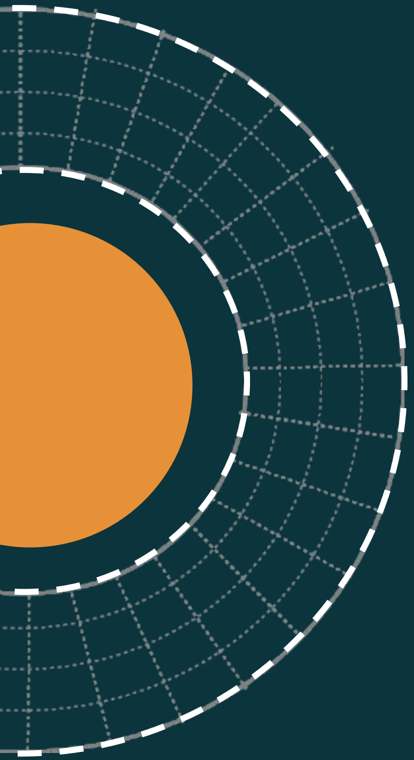

r ~ [17,157] Mm

Voxel: 2° x 2° x 14 Mm

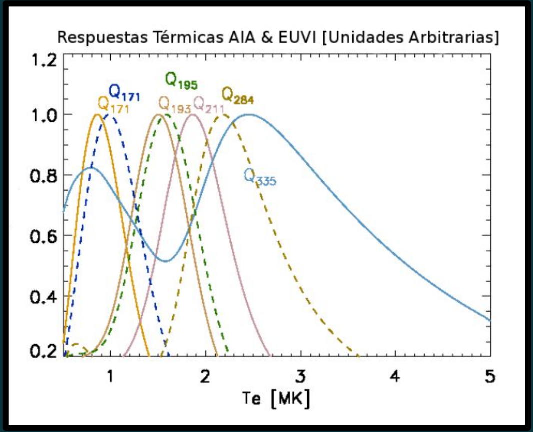

$$I_{k,j} \approx \int_{LDV} \mathrm{d}z \; \mathrm{FBE}_k(\mathbf{r}_j(z))$$

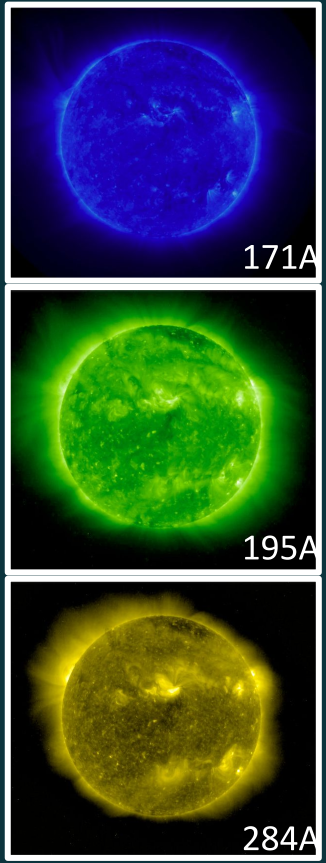

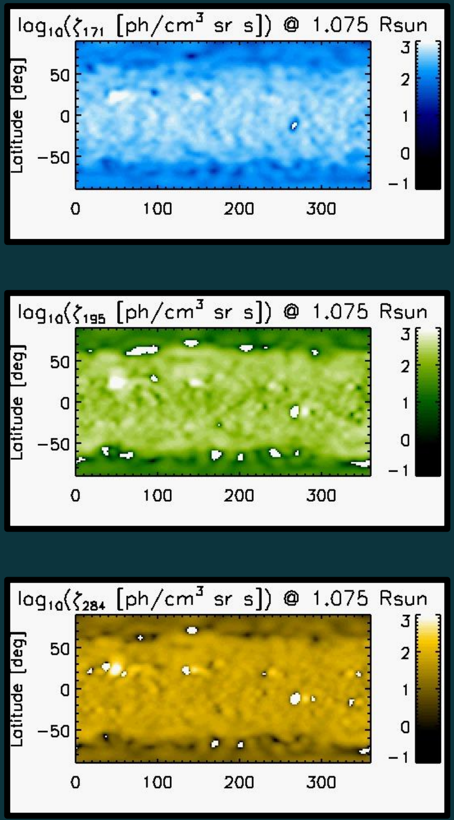

Frazin, Vásquez & Kamalabadi, 2009, ApJ, 701, p. 547.

Differential emission measure tomography technique

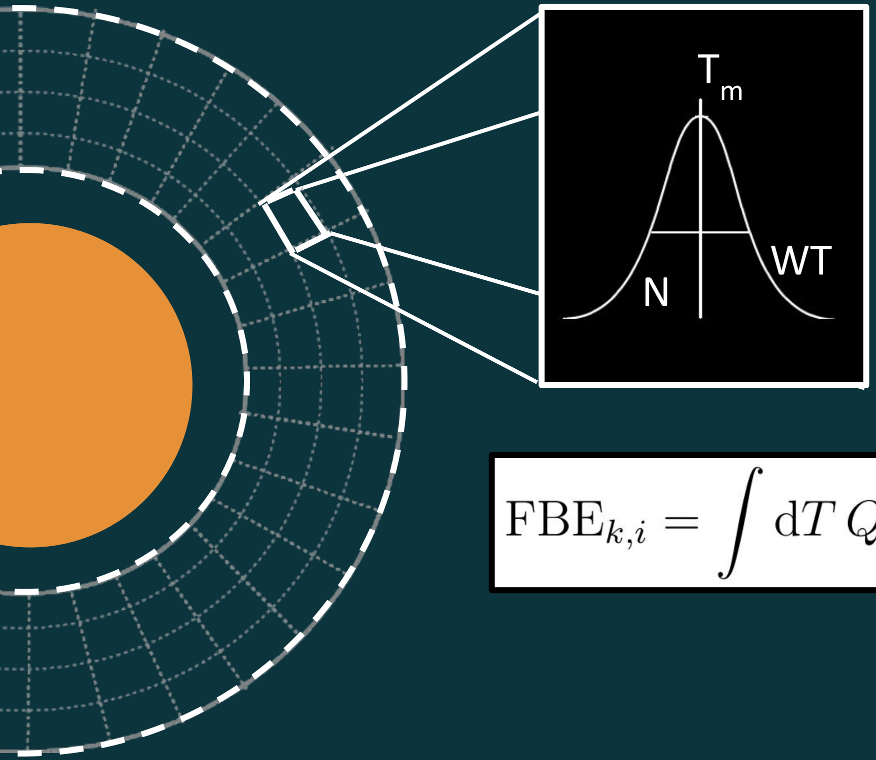

$$\mathrm{FBE}_{k,i} = \int \mathrm{d}T\, Q_k(T)\, \mathrm{LDEM}_i(T)$$

Frazin, Vásquez & Kamalabadi, 2009, ApJ, 701, p. 547.

Differential emission measure tomography technique

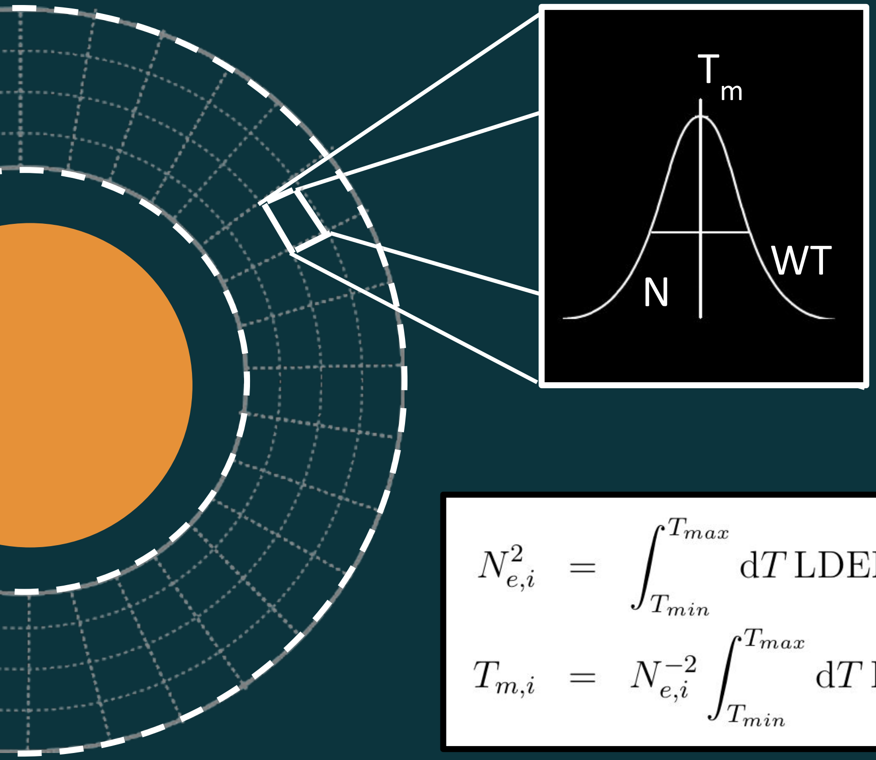

$$N_{e,i}^2 = \int_{T_{min}}^{T_{max}} \mathrm{d}T \, \mathrm{LDEM}_i(T)$$

$$T_{m,i} = N_{e,i}^{-2} \int_{T_{min}}^{T_{max}} \mathrm{d}T \, \mathrm{LDEM}_i(T) \, T$$

Frazin, Vásquez & Kamalabadi, 2009, ApJ, 701, p. 547.

Differential emission measure tomography technique

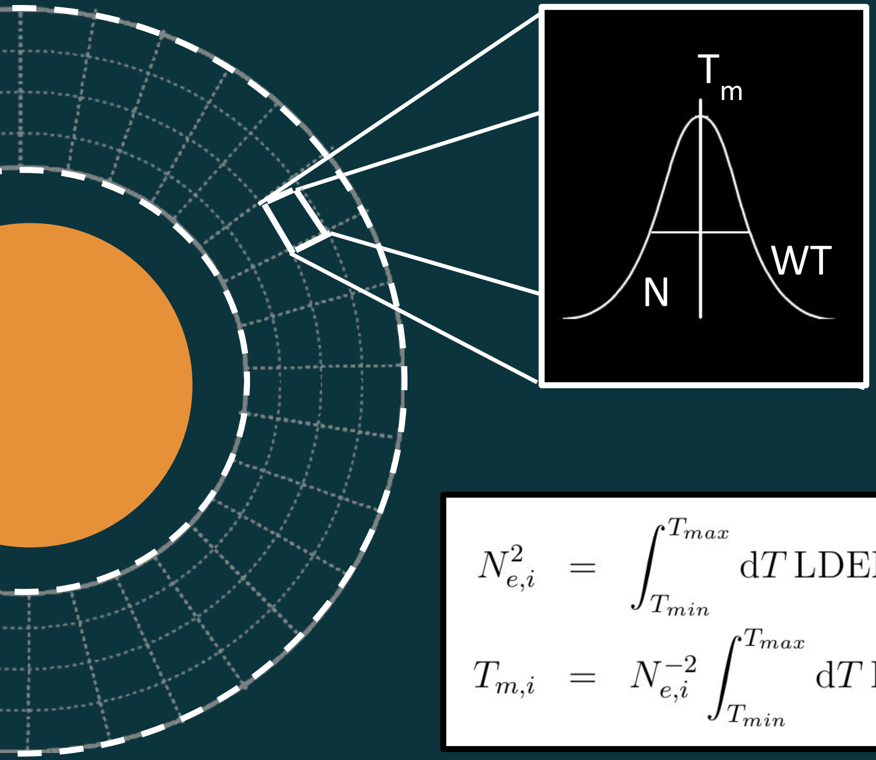

$$N_{e,i}^2 = \int_{T_{min}}^{T_{max}} \mathrm{d}T \, \mathrm{LDEM}_i(T)$$

$$T_{m,i} = N_{e,i}^{-2} \int_{T_{min}}^{T_{max}} \mathrm{d}T \, \mathrm{LDEM}_i(T) \, T$$

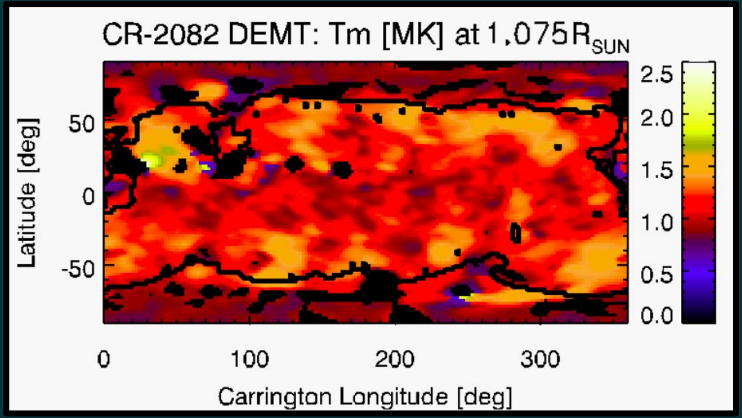

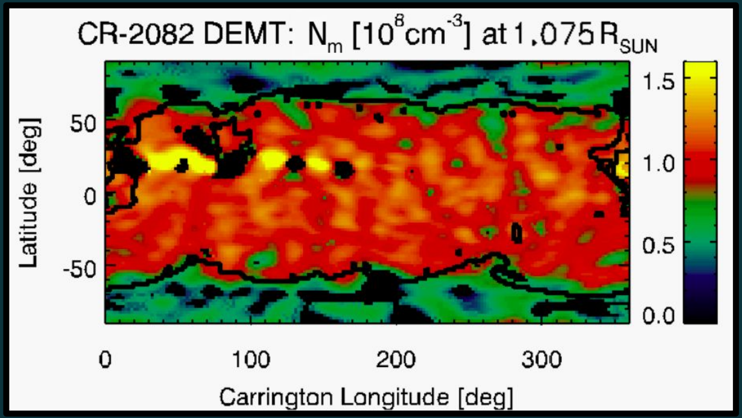

Frazin, Vásquez & Kamalabadi, 2009, ApJ, 701, p. 547.

Magnetic field extrapolation: PFSS

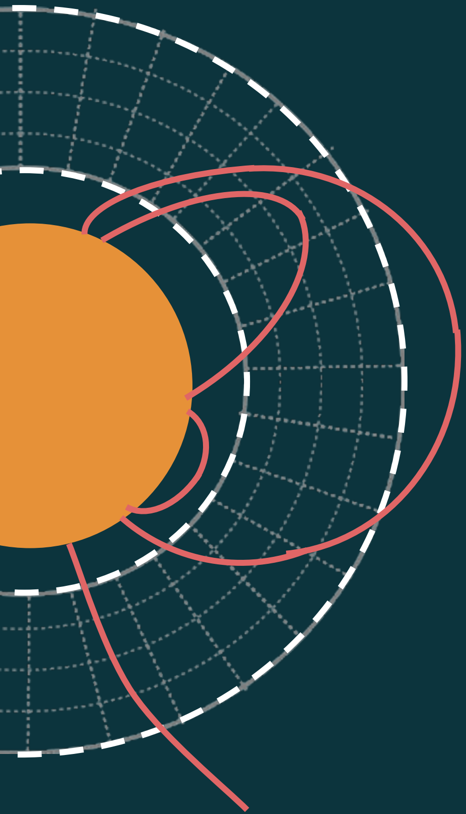

Nuevo, Vásquez, Landi & Frazin, 2015, ApJ, 811, p. 128.

Magnetic field extrapolation: PFSS

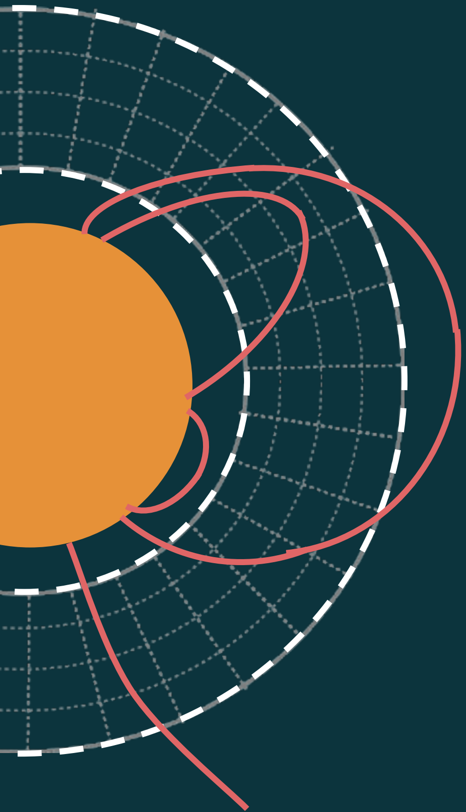

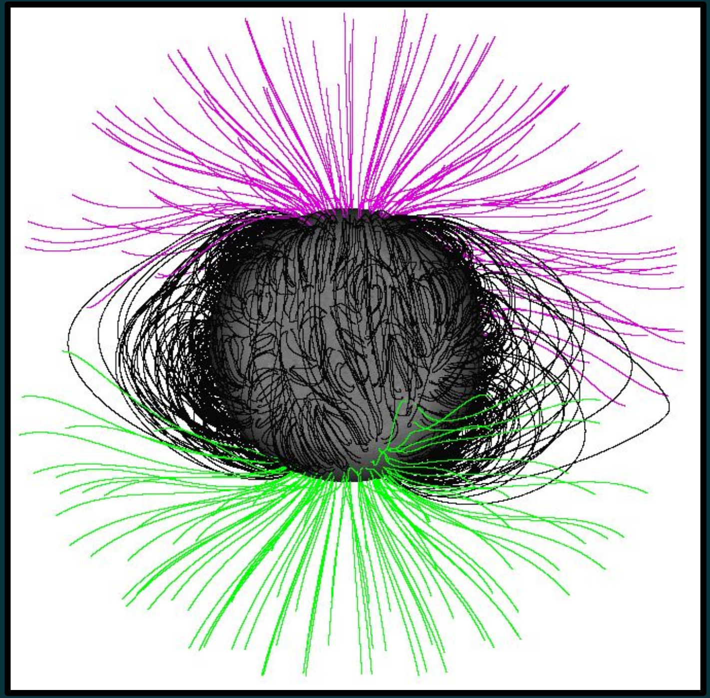

Nuevo, Vásquez, Landi & Frazin, 2015, ApJ, 811, p. 128.

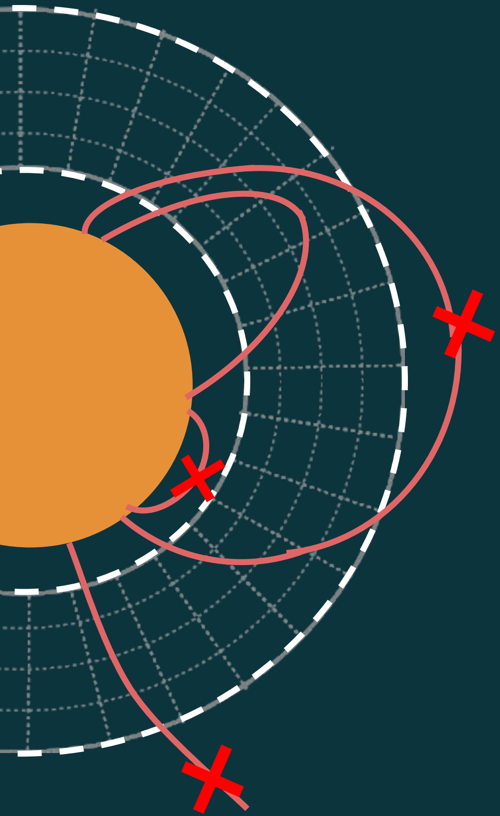

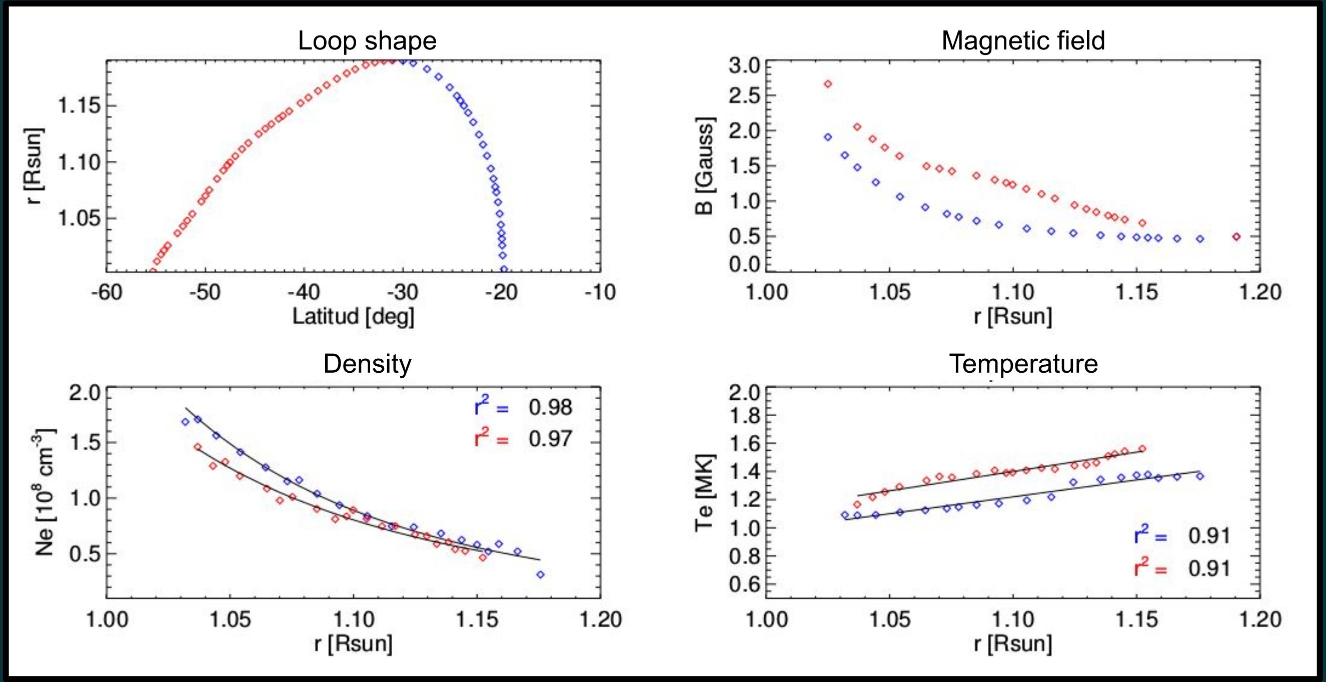

Loop shape
r [Rsun]
1.15
1.10
1.05
-60
-50
-40
-30
-20
-10
Latitud [deg]
Magnetic field
B [Gauss]
3.0
2.5
2.0
1.5
1.0
0.5
0.0
1.00
1.05
1.10
1.15
1.20
r [Rsun]
Density
Ne [10^8 cm^-3]
2.0
1.5
1.0
0.5
r^2 = 0.98
r^2 = 0.97
1.00
1.05
1.10
1.15
1.20
r [Rsun]
Temperature
Te [MK]
2.0
1.8
1.6
1.4
1.2
1.0
0.8
0.6
r^2 = 0.91
r^2 = 0.91
1.00
1.05
1.10
1.15
1.20
r [Rsun]

Quiet-Sun Typical loops

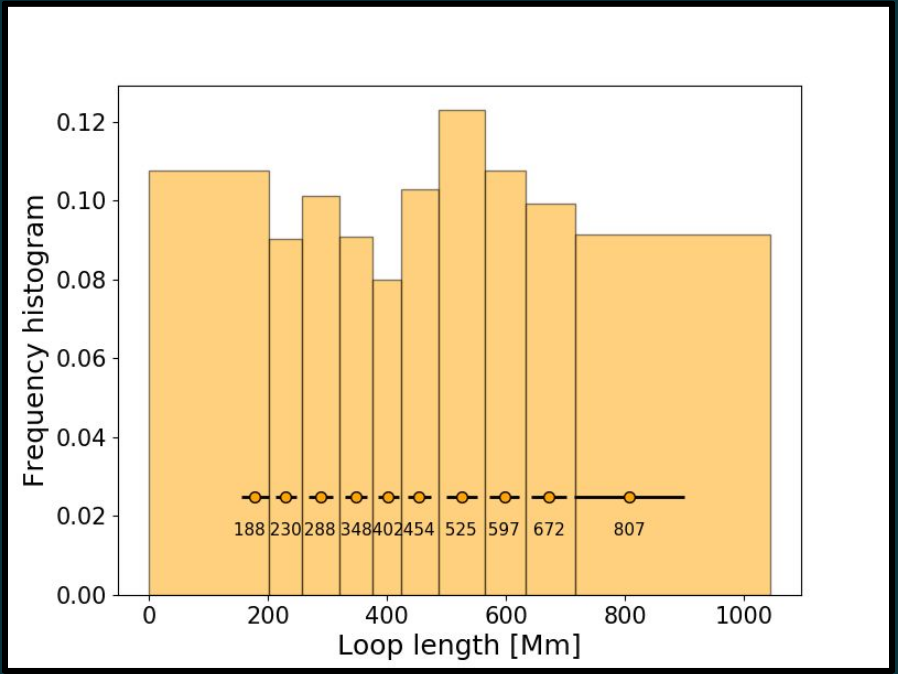

Mac Cormack et al., 2022, AdSR, 70, p. 1570.

Quiet-Sun Typical loops

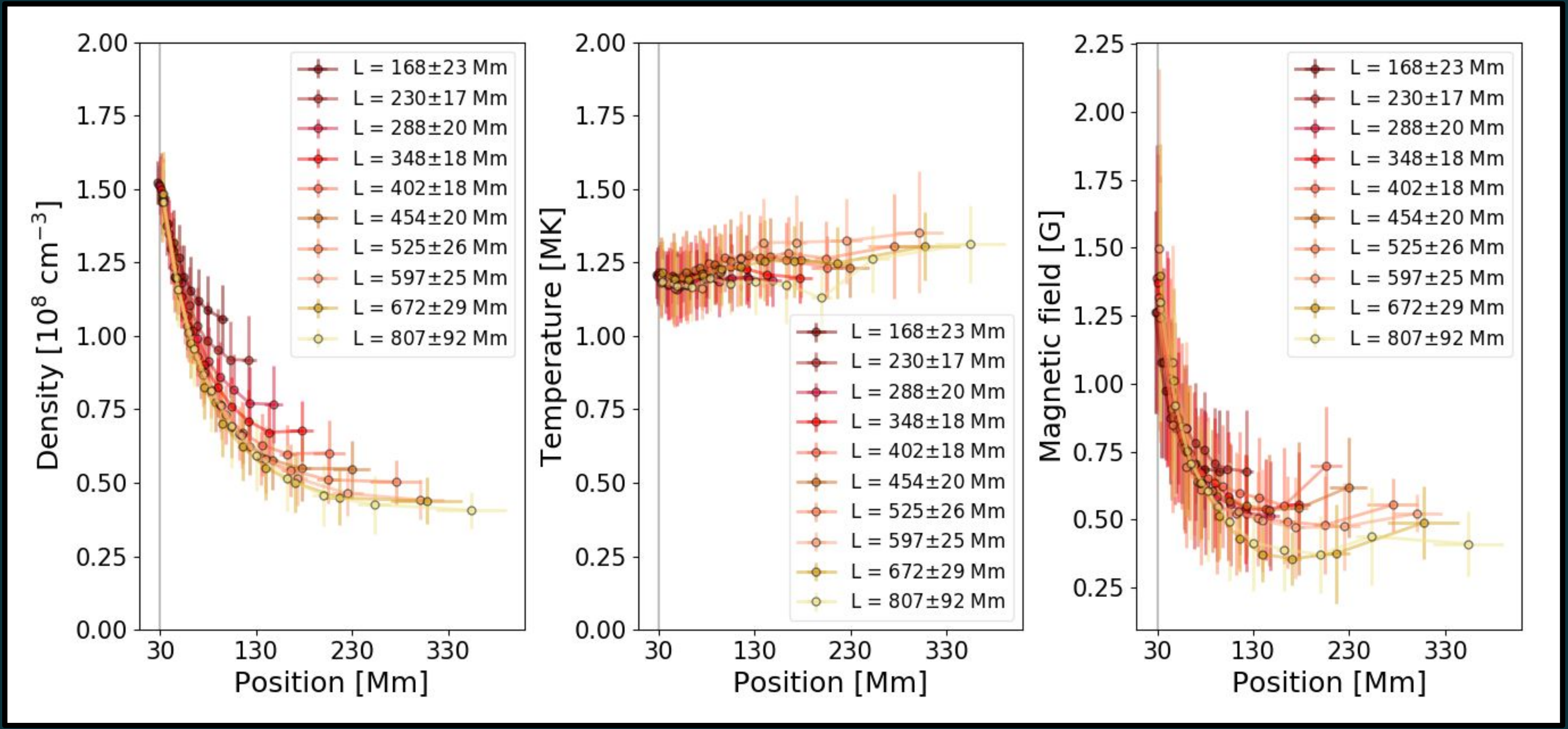

Mac Cormack et al., 2022, AdSR, 70, p. 1570.

Hydrodynamic model 0D: EBTEL

Input:

- Half loop length L/2
- Heating rate

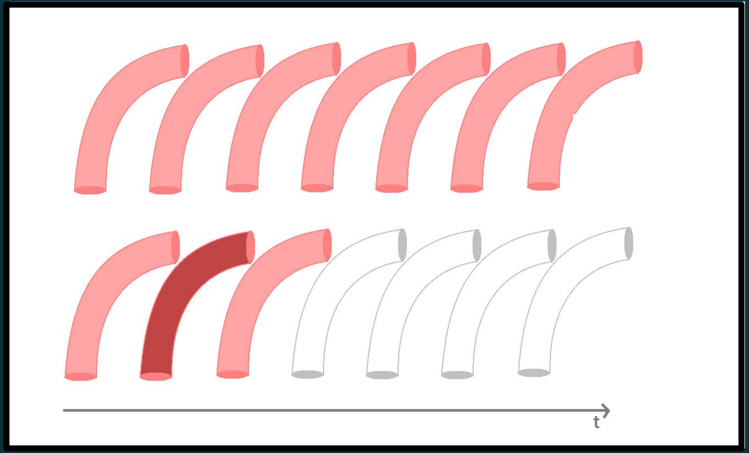

Klimchuk, Patsourakos & Cargill, 2008, ApJ, 682, p. 1351.

Hydrodynamic model 0D: EBTEL

Input:

- Half loop length L/2
- Heating rate

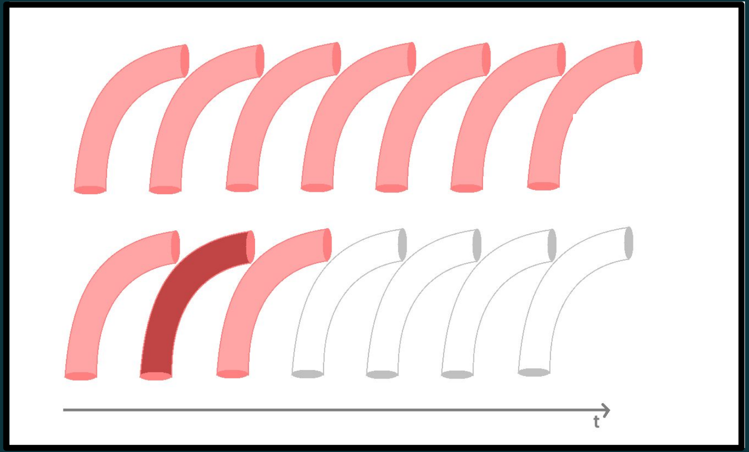

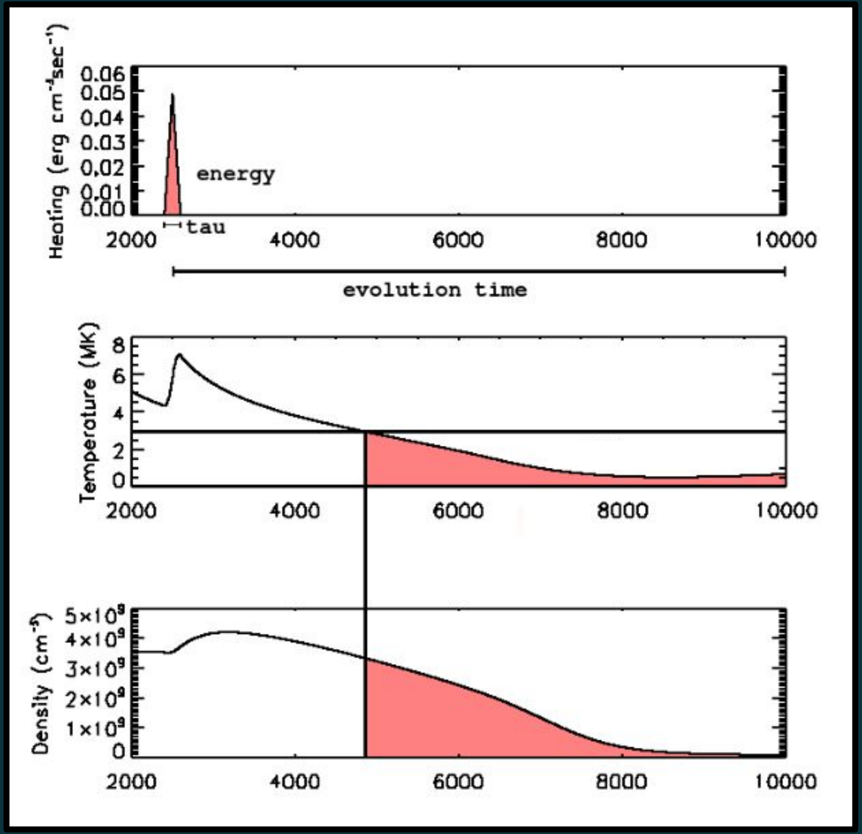

Klimchuk, Patsourakos & Cargill, 2008, ApJ, 682, p. 1351.

Quiet-Sun typical loops with EBTEL

L	$\frac{\langle N_{TL} \rangle}{\langle N_{EBTEL} \rangle_{const}}$	$\frac{\langle N_{TL} \rangle}{\langle N_{EBTEL} \rangle_{imp}}$
188	1.7	1.0
230	1.6	1.0
288	3.1	1.0
348	3.8	1.2
402	4.5	1.1
454	5.5	1.1
525	7.1	1.3
597	8.3	1.3
672	14.4	1.7
807	23.0	2.9

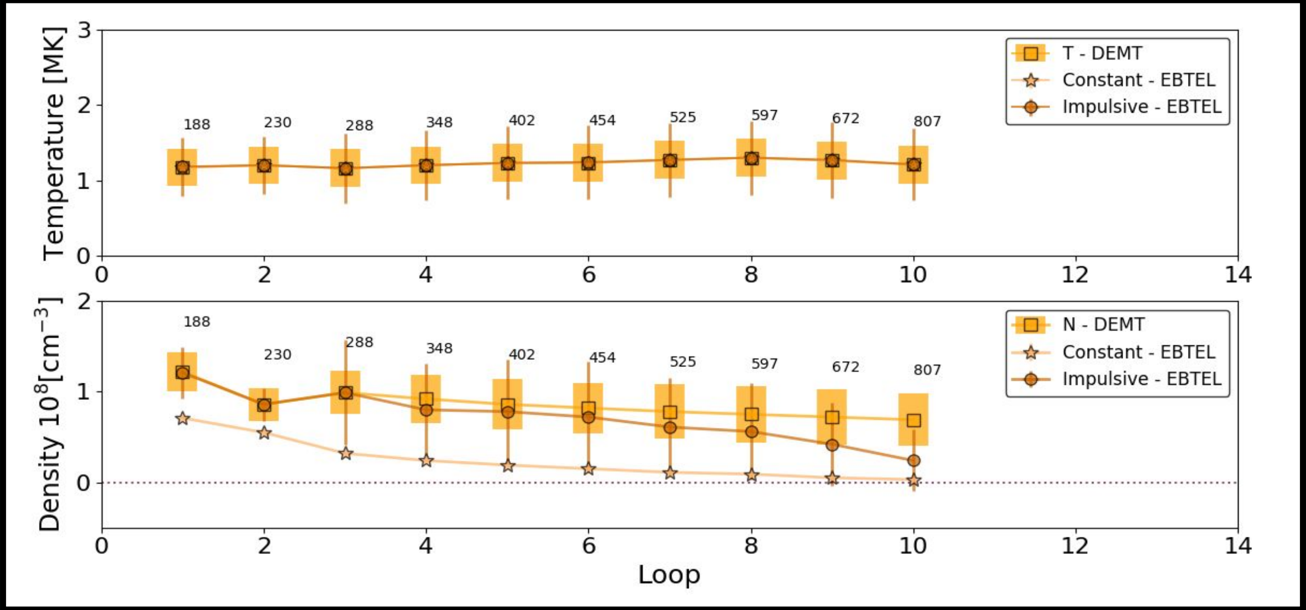

Mac Cormack et al., 2022, AdSR, 70, p. 1570.

Active regions loops with EBTEL

L [Mm]	$\frac{\langle N_e \rangle}{\langle N_e \rangle_E}$	$\frac{\langle N_e \rangle}{\langle N_e \rangle_{E_{const}}}$
137	1.04	9.0
176	1.15	18.2
128	1.14	16.3
121	0.98	9.4
208	1.13	14.4
84	1.12	9.2
93	0.83	5.0
132	0.94	8.1
337	1.45	60.8
195	1.02	10.3
353	0.36	161.2
175	1.06	23.5
163	1.21	28.2

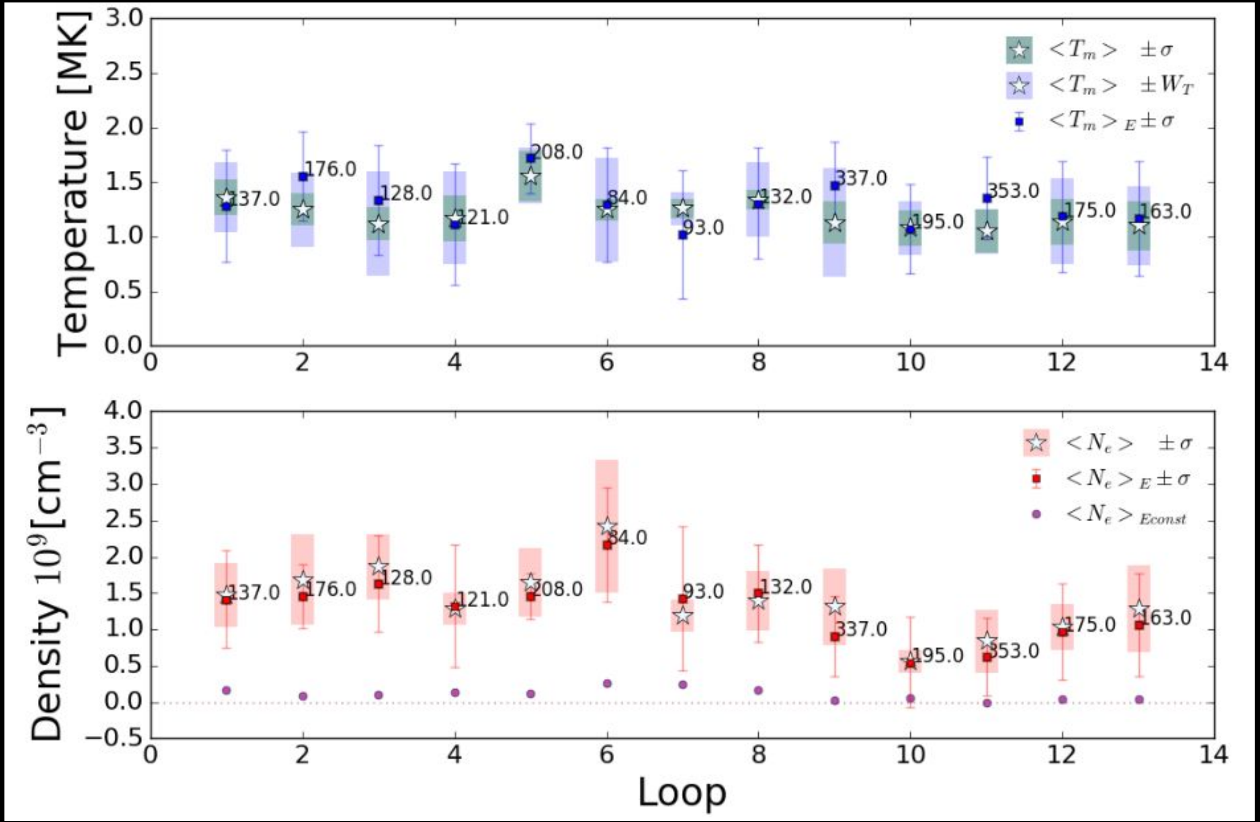

Nuevo et al., 2020, SoPh, 295, p. 1570.

Hydrodynamic model 1D: HYDRAD

Input:

Loop length

Volumetric heating rate: temporal and spatial profile.

Chromosphere depth: 5 Mm

Foot-point values of:

Temperatura 20000 K

Densidad 10^{10} cm^{-3}

(Vernazza et al. 1981, ApJ, 45, 635-725).

Bradshaw & Cargill, 2013, ApJ, 770, p. 13.

Hydrodynamic model 1D: HYDRAD

Input:

Loop length

Volumetric heating rate: temporal and spatial profile.

Chromosphere depth: 5 Mm

Foot-point values of:

Temperatura 20000 K

Densidad 10^{10} cm^{-3}

(Vernazza et al. 1981, ApJ, 45, 635-725).

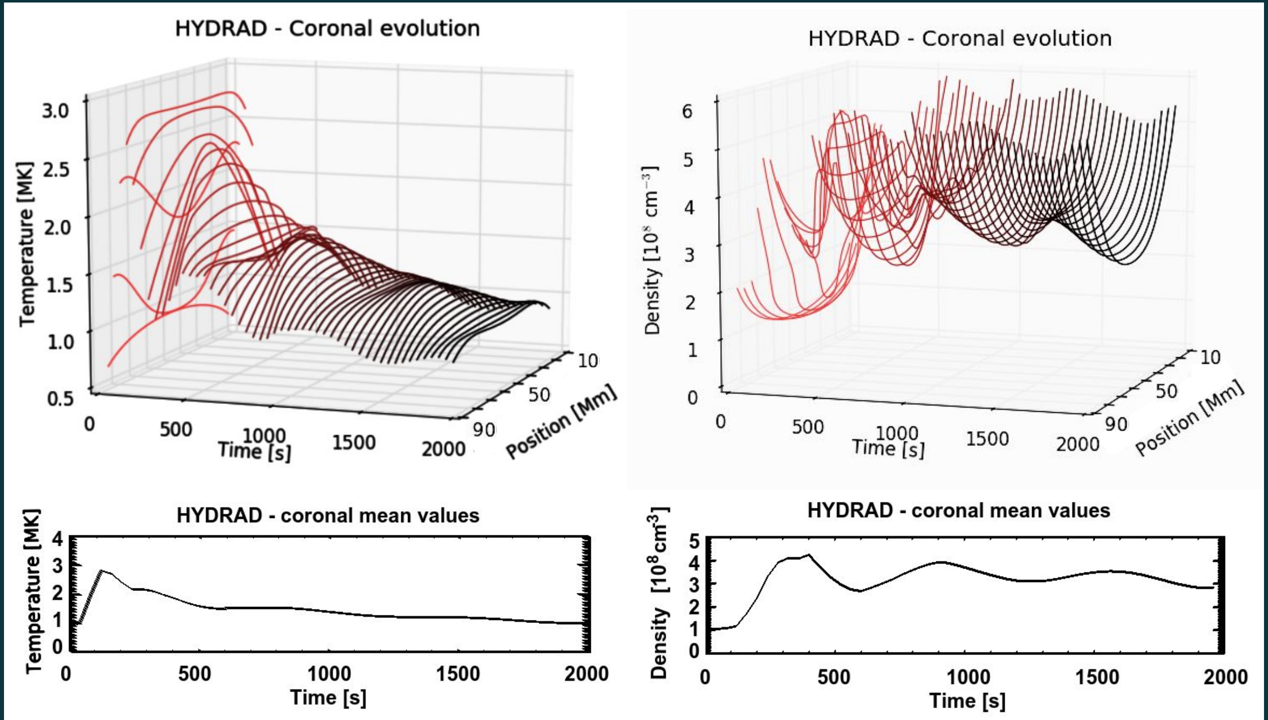

Bradshaw & Cargill, 2013, ApJ, 770, p. 13.

Quiet-Sun typical loops with HYDRAD

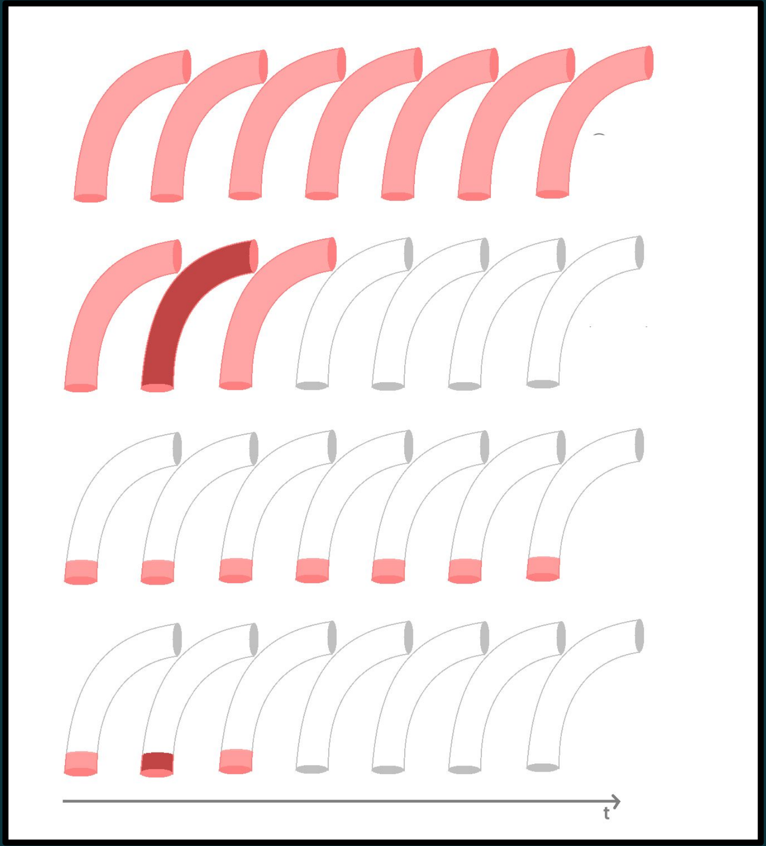

Mac Cormack et al 2023, in preparation

Quiet-Sun typical loops with HYDRAD

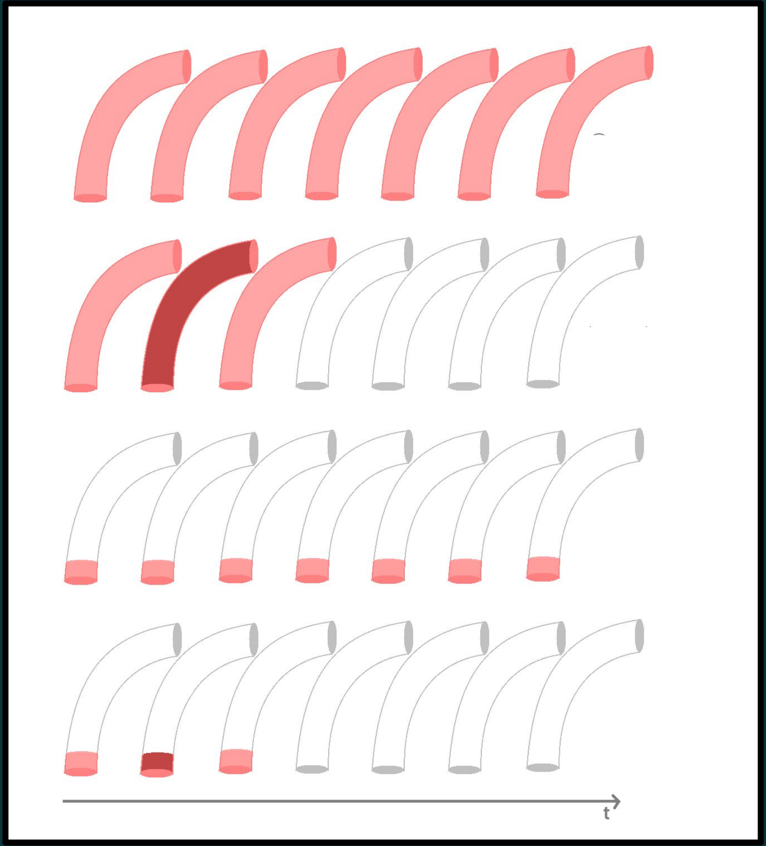

$$E_{N,T} = \left\langle \frac{|\mathrm{HYDRAD_{N,T}} - \mathrm{DEMT_{N,T}}|}{\mathrm{DEMT_{N,T}}} \right\rangle$$

$$E_M = \langle E_N, E_T \rangle$$

Mac Cormack et al 2023, in preparation

Typical loops: constant and uniform heating

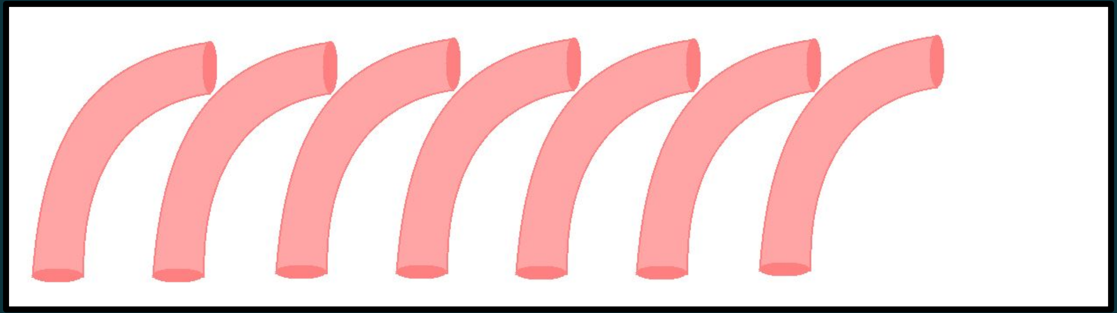

Mac Cormack et al 2023, in preparation

Typical loops: constant and uniform heating

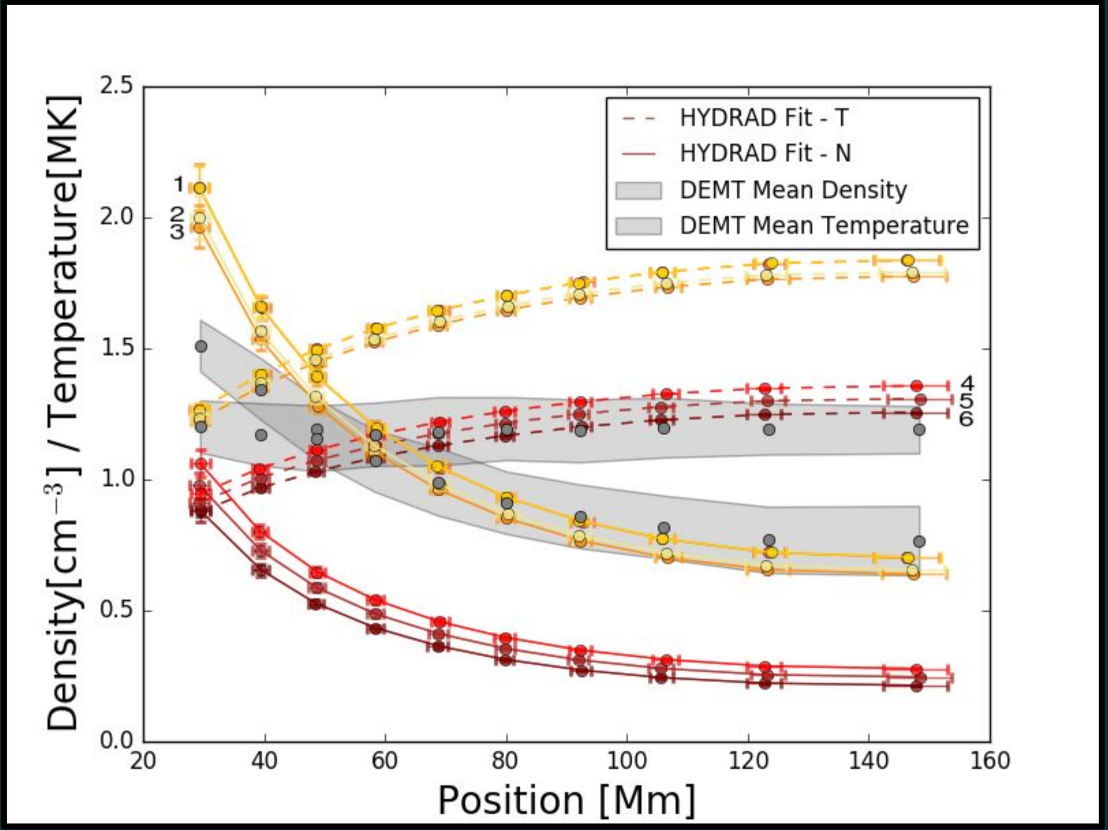

Mac Cormack et al 2023, in preparation

Typical loops: constant and uniform heating

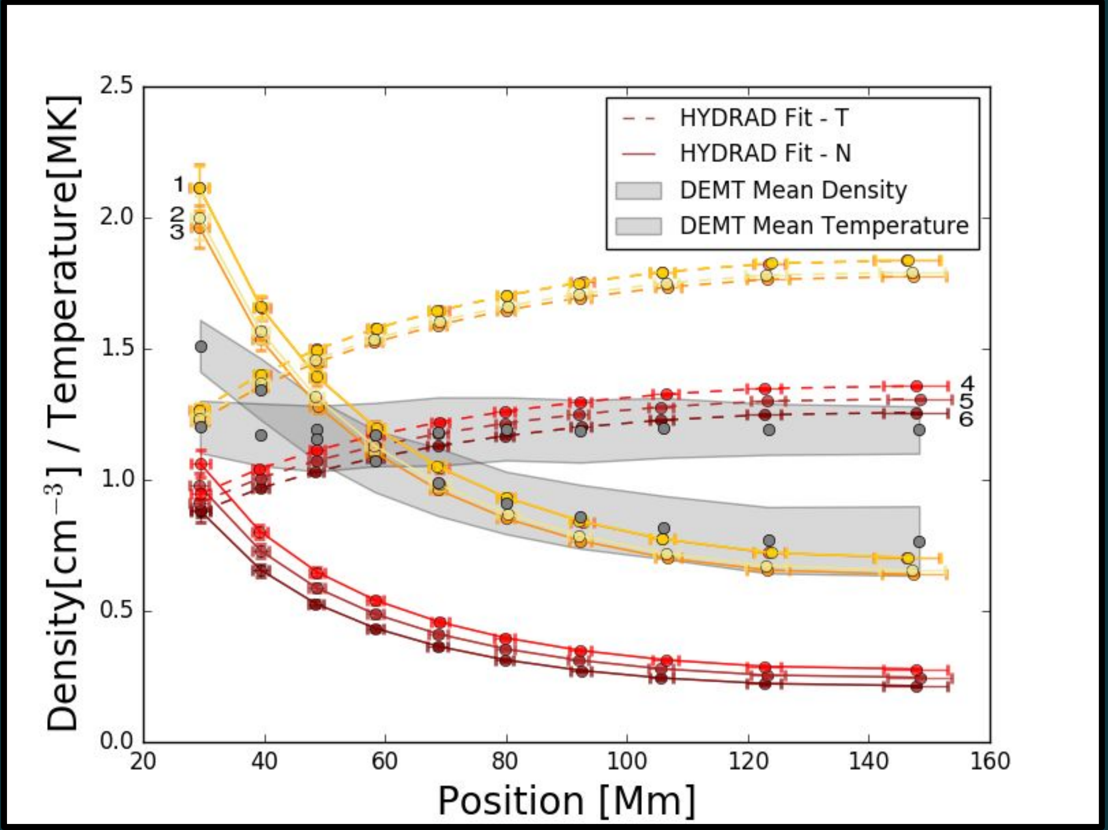

$Error$	1	2	3	4	5	6
E_N	0.12	0.12	0.12	0.52	0.57	0.62
E_T	0.37	0.34	0.33	0.09	0.08	0.08
E_M	0.25	0.23	0.23	0.31	0.33	0.35

Density: $[0.5-3]\times10^{10}$ cm^{-3}
Temperature: $[1.6\text{-}2.4]\times10^{4}$ K
Volumetric heating peak: $[0.2-4]\times10^{-6}$ erg cm^{-3} s^{-1}

Mac Cormack et al 2023, in preparation

Typical loops: impulsive and uniform heating

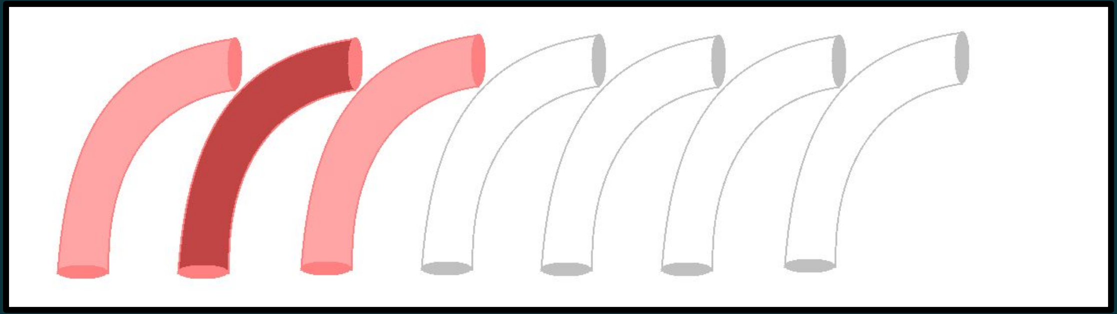

Mac Cormack et al 2023, in preparation

Typical loops: impulsive and uniform heating

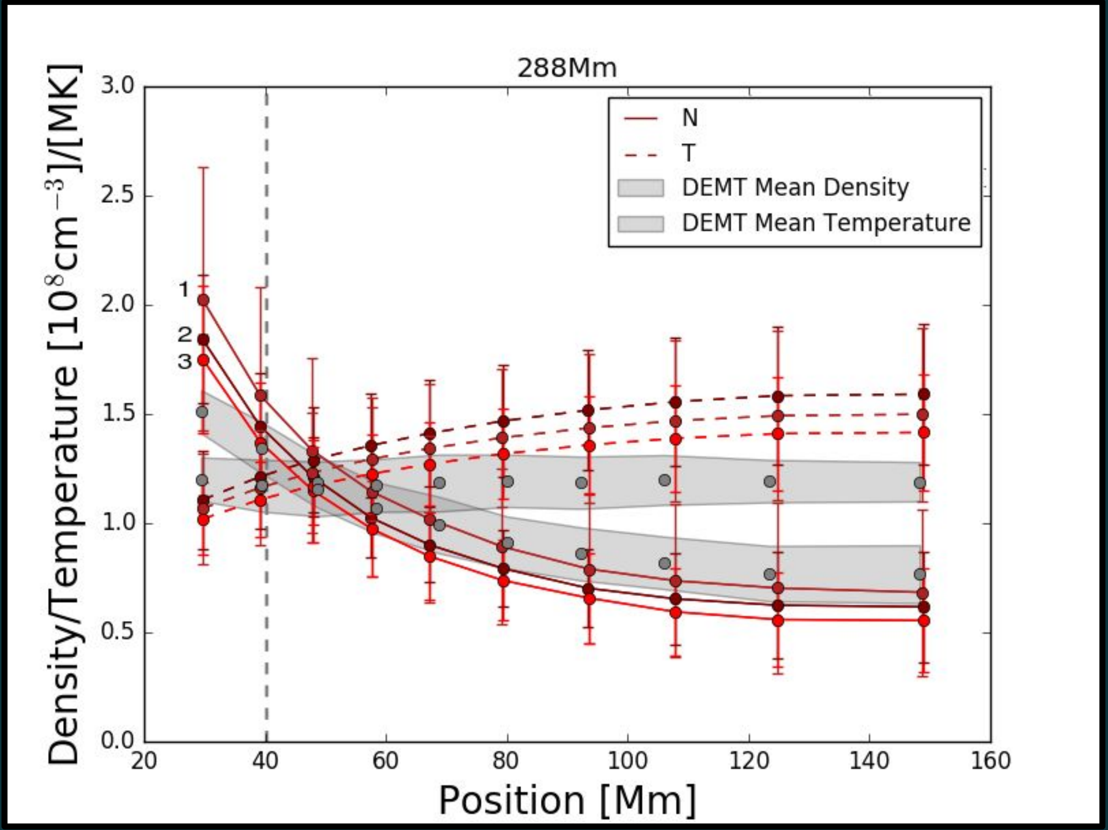

Mac Cormack et al 2023, in preparation

Typical loops: impulsive and uniform heating

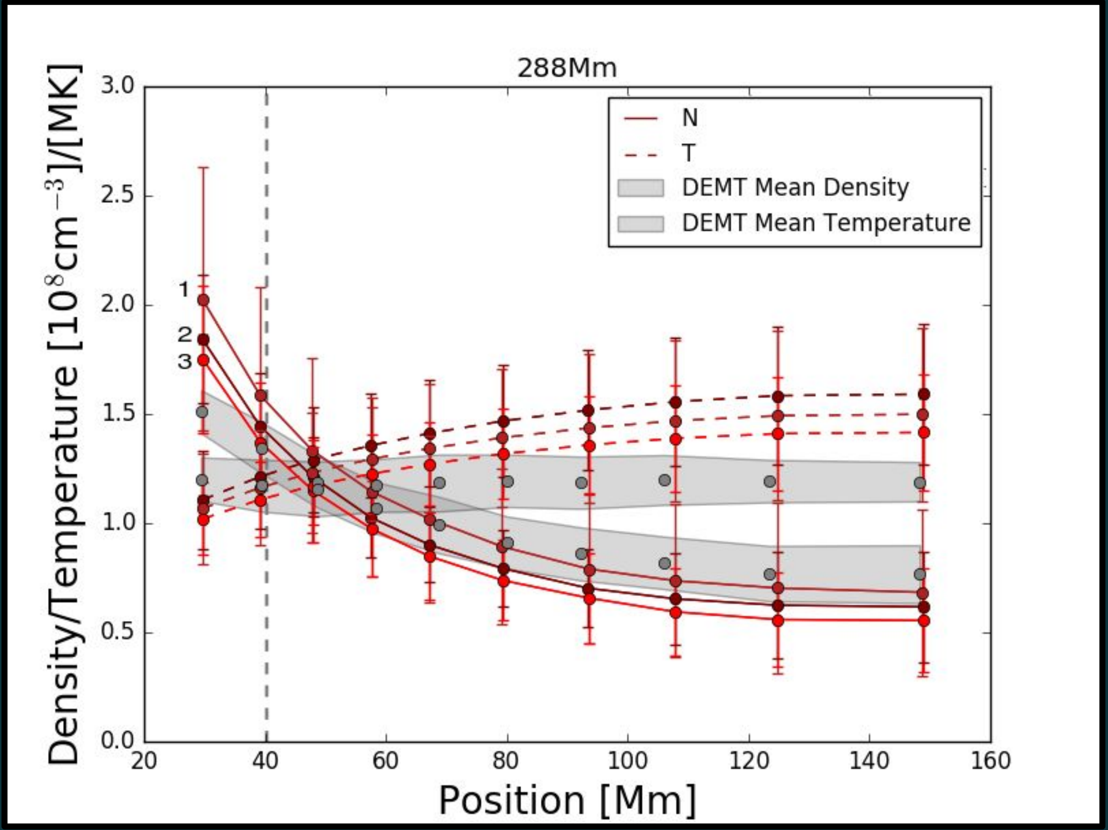

$L[Mm]$	E_N	E_T	E_M	E_{N2}	E_{T2}	E_{M2}
188	0.11	0.06	0.09	0.07	0.04	0.05
230	0.15	0.09	0.12	0.08	0.09	0.09
288	0.11	0.15	0.13	0.08	0.18	0.13
348	0.20	0.16	0.18	0.22	0.18	0.20
402	0.17	0.21	0.19	0.17	0.25	0.21
454	0.35	0.15	0.25	0.41	0.17	0.29
525	0.35	0.19	0.27	0.42	0.23	0.33
597	0.35	0.20	0.28	0.42	0.23	0.33
672	0.57	0.17	0.37	0.63	0.19	0.41
807	0.60	0.25	0.42	0.67	0.29	0.48

Duration: [50−500] s

Volumetric heating peak: [10^{-4}-10^{-3}] erg cm^{-3} s^{-1}

Energy input: [3×10^5-7×10^5] erg cm^{-2} s^{-1}

Mac Cormack et al 2023, in preparation

Typical loops: constant and localized heating

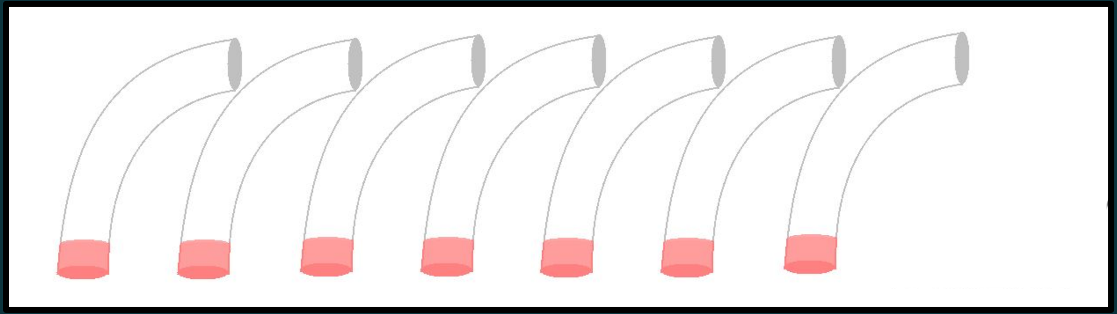

Mac Cormack et al 2023, in preparation

Typical loops: constant and localized heating

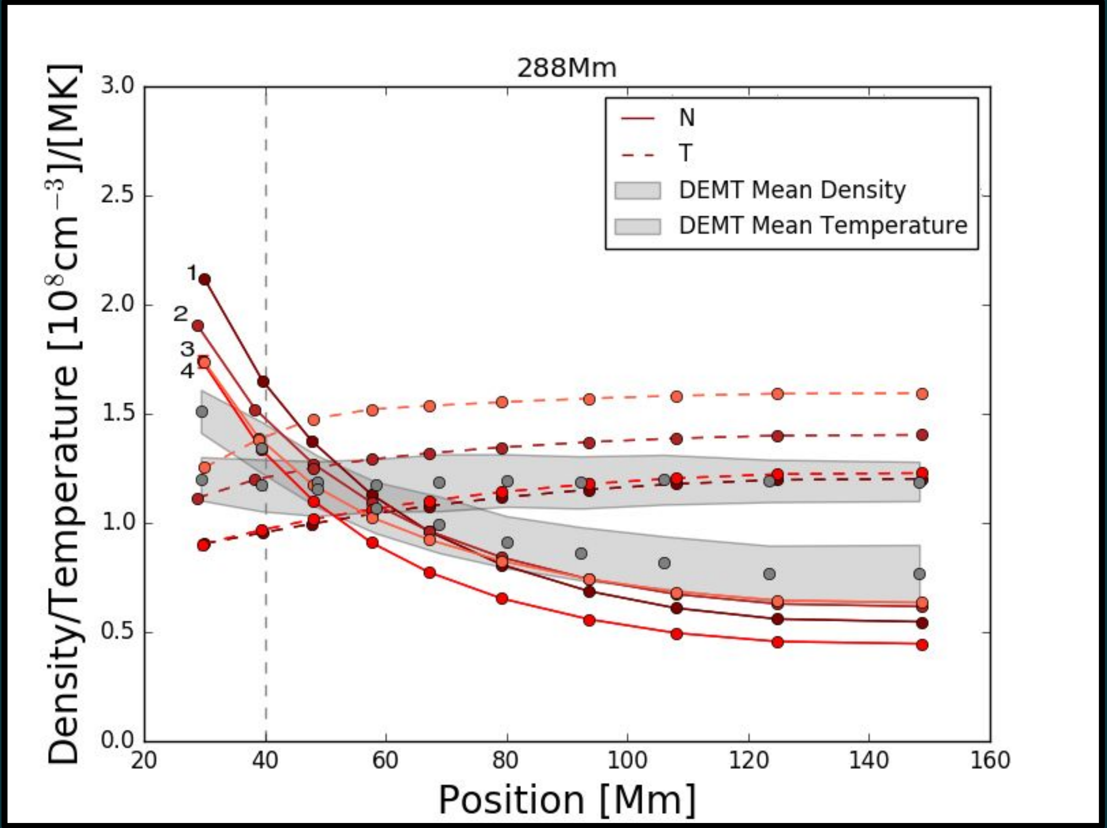

Mac Cormack et al 2023, in preparation

Typical loops: constant and localized heating

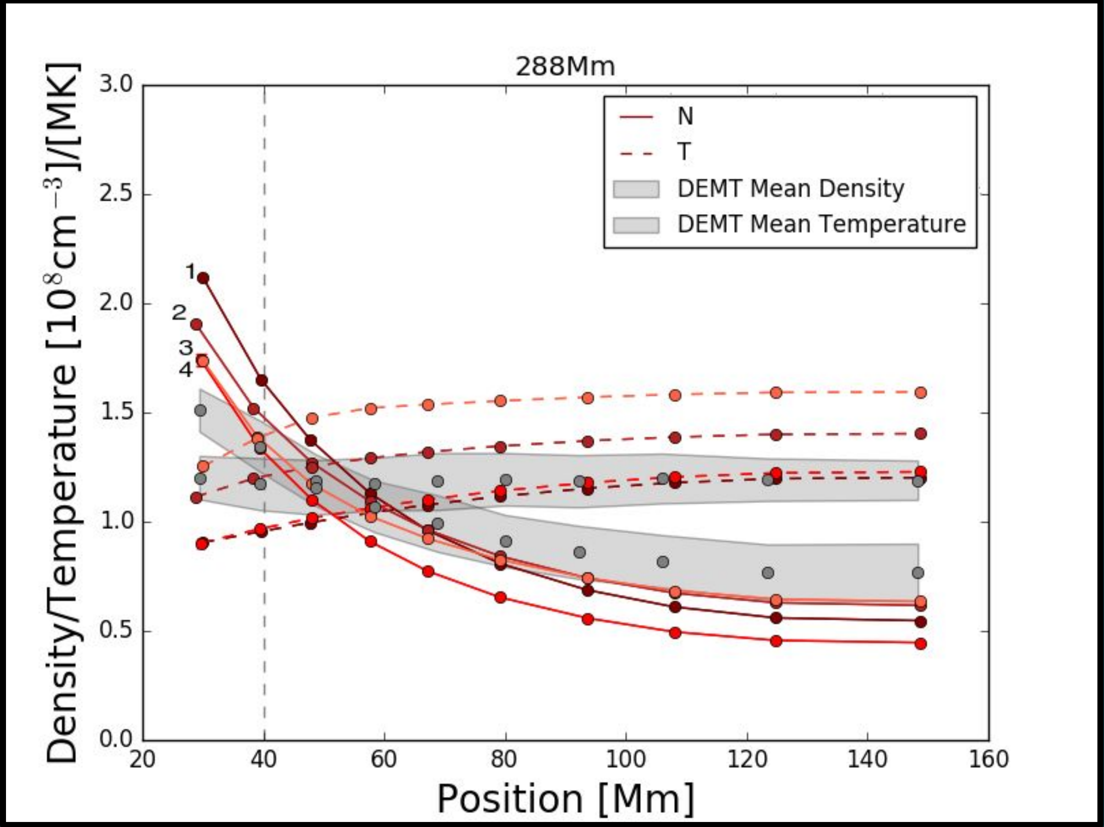

$L[Mm]$	E_N	E_T	E_M	E_{N2}	E_{T2}	E_{M2}
188	0.09	0.04	0.07	0.07	0.03	0.05
230	0.14	0.08	0.11	0.10	0.05	0.08
288	0.13	0.12	0.12	0.11	0.14	0.12
348	0.14	0.16	0.15	0.10	0.18	0.14
402	0.25	0.08	0.16	0.19	0.07	0.13
454	0.18	0.17	0.17	0.16	0.20	0.18
525	0.21	0.18	0.20	0.22	0.22	0.22
597	0.34	0.10	0.22	0.27	0.08	0.18
672	0.33	0.13	0.23	0.32	0.13	0.23
807	0.31	0.27	0.29	0.35	0.32	0.33

Spatial scale: [5−30] Mm
Volumetric heating peak: [10^{-5}-3×10^{-4}] erg cm^{-3} s^{-1}

Energy input: [1×10^5-1.5×10^5] erg cm^{-2} s^{-1}

Mac Cormack et al 2023, in preparation

Typical loops: impulsive and localized heating

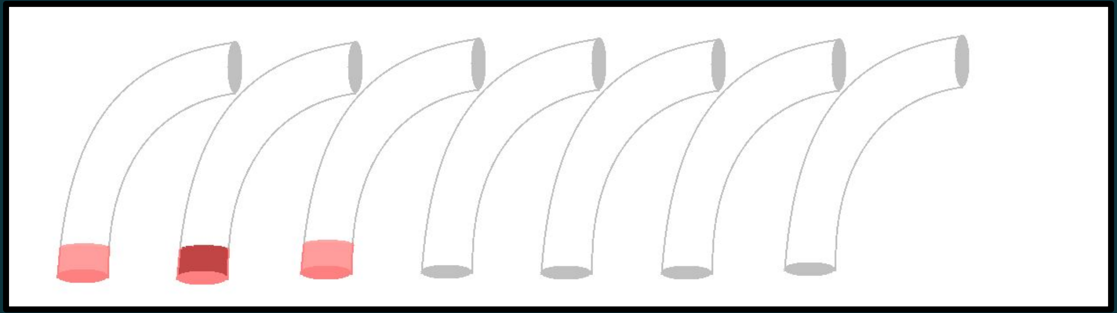

Mac Cormack et al 2023, in preparation

Typical loops: impulsive and localized heating

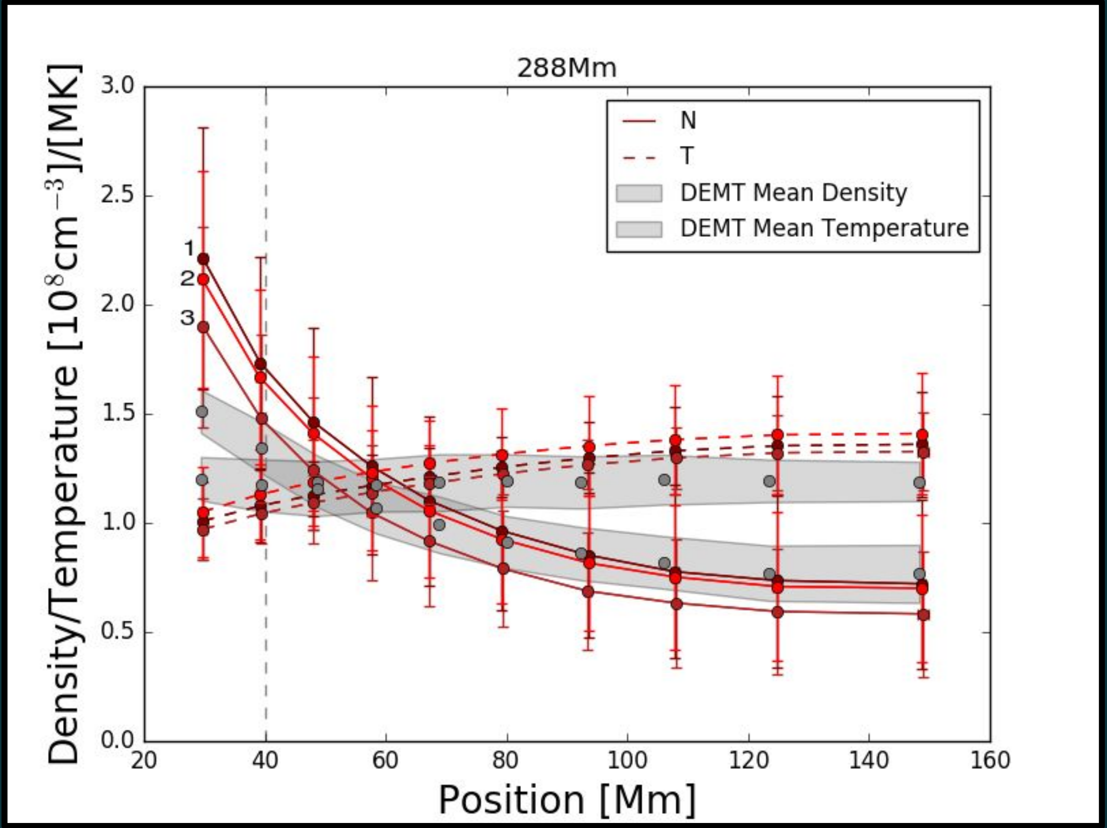

Mac Cormack et al 2023, in preparation

Typical loops: impulsive and localized heating

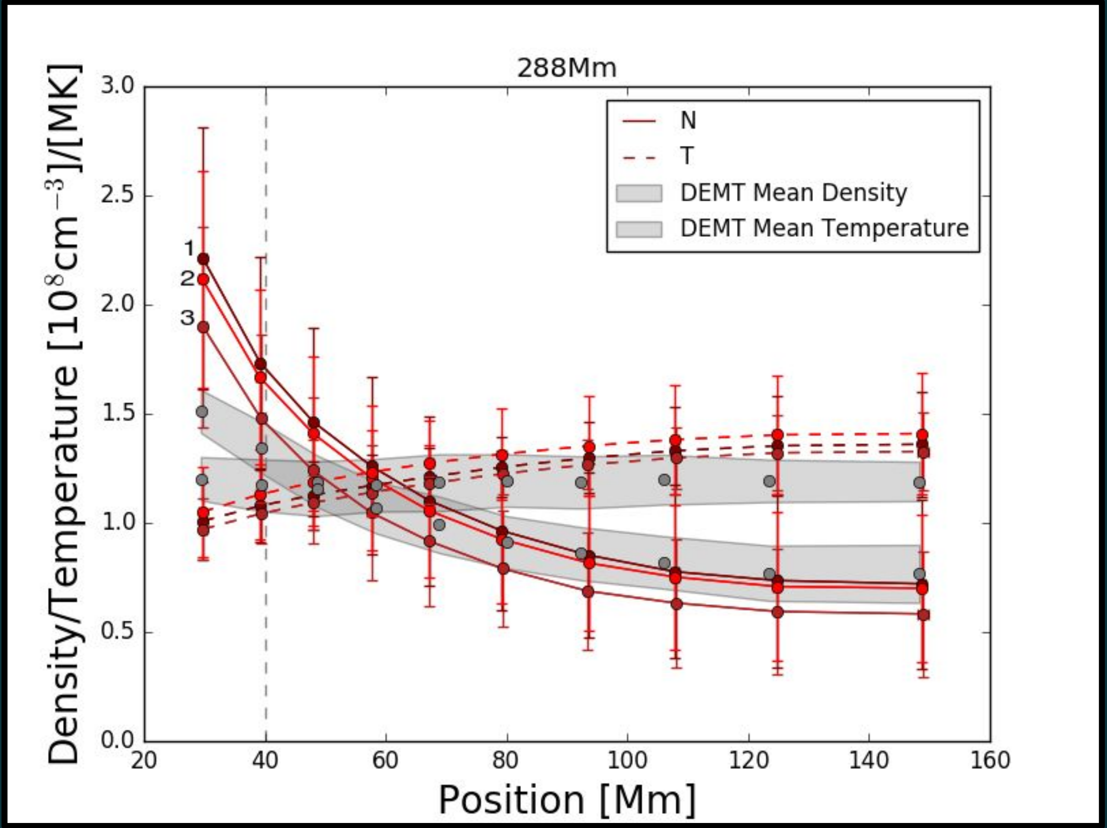

$L[Mm]$	E_N	E_T	E_M	E_{N2}	E_{T2}	E_{M2}
188	0.09	0.04	0.07	0.07	0.03	0.05
230	0.12	0.07	0.09	0.09	0.04	0.06
288	0.15	0.08	0.12	0.09	0.07	0.08
348	0.15	0.10	0.13	0.10	0.10	0.10
402	0.18	0.10	0.14	0.14	0.10	0.12
454	0.20	0.11	0.15	0.16	0.11	0.13
525	0.24	0.12	0.18	0.22	0.12	0.17
597	0.27	0.12	0.19	0.26	0.12	0.19
672	0.28	0.14	0.21	0.28	0.15	0.22
807	0.33	0.20	0.26	0.35	0.23	0.29

Duration: [100-500] s
Spatial scale: [5−100] Mm
Spatial location: 5 Mm
Volumetric heating peak: [5×10^{-4}-0.1] erg cm^{-3} s^{-1}

Energy input: [0.7×10^{5}-1.1×10^{5}] erg cm^{-2} s^{-1}

Mac Cormack et al 2023, in preparation

Summary

Summary

- We study scaling laws in quiet-Sun coronal loops. (Mac Cormack et al. 2020, AdSpR, Volume 65, Issue 6, p. 1616-1628.)

Summary

- We study scaling laws in quiet-Sun coronal loops. (Mac Cormack et al. 2020, AdSpR, Volume 65, Issue 6, p. 1616-1628.)

- We construct typical loops of the quiescent corona and we model them with HD models assuming different heating scenarios.

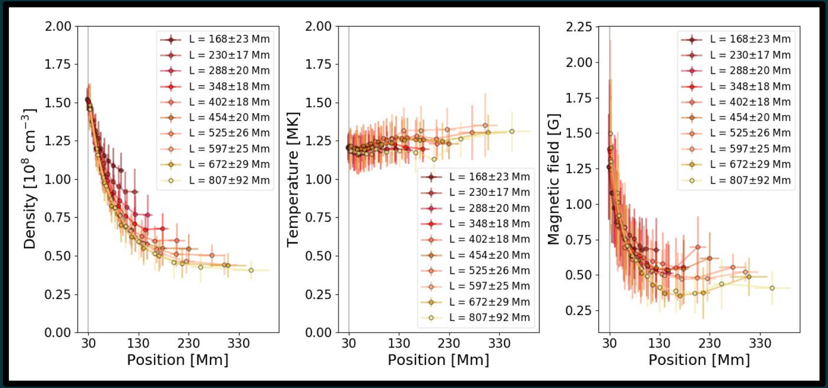

Summary

- We study scaling laws in quiet-Sun coronal loops. (Mac Cormack et al. 2020, AdSpR, Volume 65, Issue 6, p. 1616-1628.)

- We construct typical loops of the quiescent corona and we model them with HD models assuming different heating scenarios.

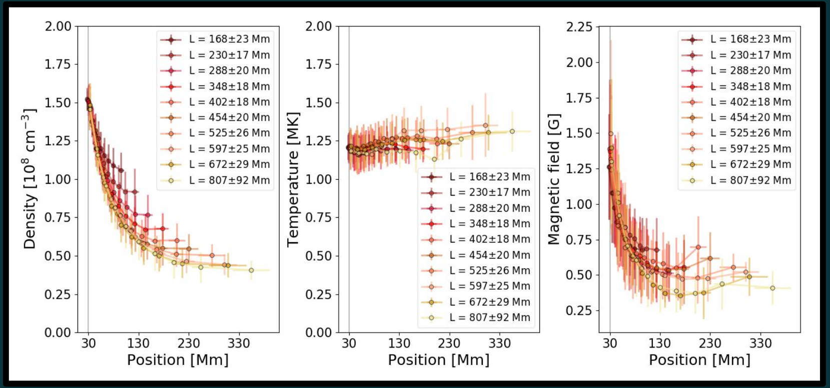

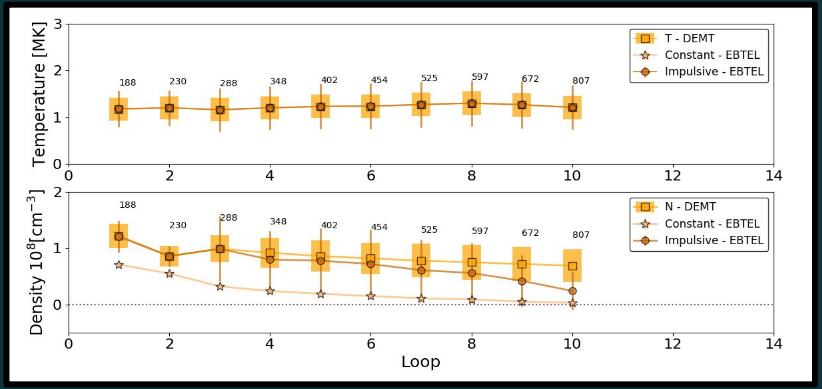

0D model: EBTEL (Klimchuk et al. 2008, ApJ, 682:1351-1362)

We found that average density and temperature are well reproduced when we assume an impulsive heating scenario in short coronal loops (Mac Cormack et al 2022, AdSpR, Volume 70, Issue 6, p. 1570-1579.)

Summary

- We study scaling laws in quiet-Sun coronal loops. (Mac Cormack et al. 2020, AdSpR, Volume 65, Issue 6, p. 1616-1628.)

- We construct typical loops of the quiescent corona and we model them with HD models assuming different heating scenarios.

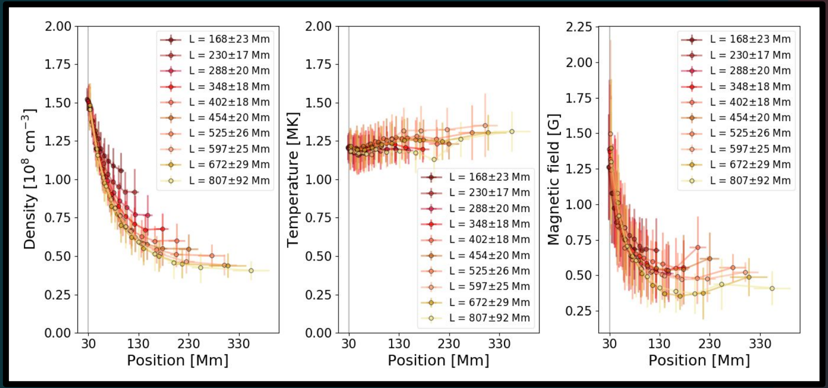

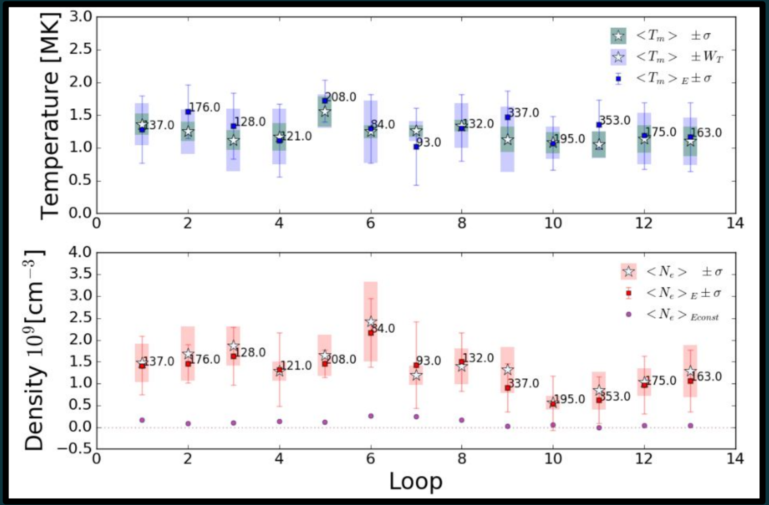

0D model: EBTEL (Klimchuk et al. 2008, ApJ, 682:1351-1362)
We found that average density and temperature are well reproduced when we assume an impulsive heating scenario in short coronal loops (Mac Cormack et al 2022, AdSpR, Volume 70, Issue 6, p. 1570-1579.)

We found the same result for active regions loops (Nuevo et al. 2020, SoPh, Volume 295, Issue 12, article id.171)

Summary

1D model: HYDRAD (Bradshaw & Cargill, 2013, ApJ, 770, p. 13.)
We found that the error is less than 15% in both density and temperature for semicircular loops. (Mac Cormack et al 2023, in preparation)

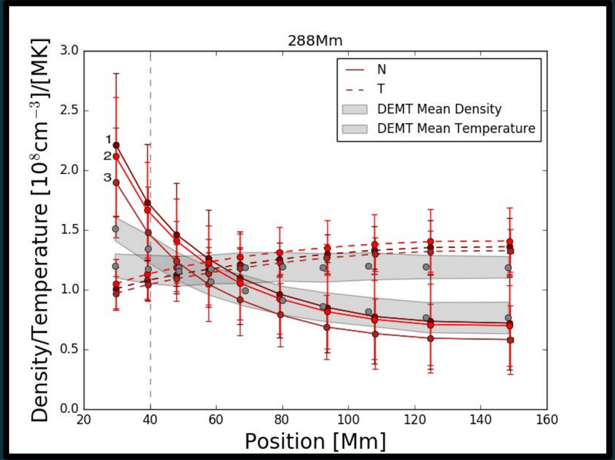

We found that localized heating (both impulsive and constant) at the coronal base is the best scenario to reproduce the thermal properties reconstructed with the tomography technique.

Thank you!